

Molecular Imaging of Pulmonary Inflammation in Electronic and Combustible Cigarette

Users: A Pilot Study

Reagan R. Wetherill^{1*}, Robert K. Doot², Anthony J. Young², Hsiaoju Lee², Erin K. Schubert²,
Corinde E. Wiers^{1,2}, Frank T. Leone³, Robert H. Mach², Henry R. Kranzler^{1,4}, Jacob G. Dubroff²

¹ Department of Psychiatry, Perelman School of Medicine, University of Pennsylvania, Philadelphia, PA, USA

² Department of Radiology, Perelman School of Medicine, University of Pennsylvania, Philadelphia, PA, USA

³ Comprehensive Smoking Treatment Program, Penn Lung Center, Philadelphia, PA, USA

⁴ Crescenz VAMC, Philadelphia, PA, USA.

Corresponding Author: *Reagan R. Wetherill, Ph.D., 3535 Market Street, Suite 500,

Philadelphia, PA 19104, rweth@penncmedicine.upenn.edu, +1(215)746-3953

Word Count: 4,967

Figures: 3 (+2 Supplementary)

Running Title: FNOS PET PULMONARY INFLAMMATION

Immediate Open Access: Creative Commons Attribution 4.0 International License (CC BY) allows users to share and adapt with attribution, excluding materials credited to previous publications.

License: <https://creativecommons.org/licenses/by/4.0/>.

Details: <https://jnm.snmjournals.org/page/permissions>.



ABSTRACT

Electronic cigarette (EC) use has increased dramatically, particularly among adolescents and young adults, which, like cigarette use, can cause pulmonary inflammation and increase the risk of lung disease. **Methods:** This preliminary study used positron emission tomography with ^{18}F -6-(1/2)(2-fluoro-propyl)-4-methylpyridin-2-amine (^{18}F -NOS) to quantify inducible nitric oxide synthase (iNOS) expression to characterize oxidative stress and inflammation in the lungs *in vivo* in three age- and sex-matched groups: (1) 5 EC users, (2) 5 cigarette smokers, and (3) 5 never smoke/vape controls. **Results:** EC users showed greater ^{18}F -NOS non-displaceable binding potential (BP_{ND}) than cigarette smokers ($p= 0.03$) and never smoke/vape controls ($p= 0.01$); whereas BP_{ND} in cigarette smokers did not differ from controls ($p> 0.1$). ^{18}F -NOS lung tissue delivery and iNOS distribution volume did not significantly differ between groups. Although there were no group differences in peripheral inflammatory biomarker concentrations, ^{18}F -NOS BP_{ND} correlated with the pro-inflammatory cytokine tumor necrosis factor- α concentrations ($r_s= 0.87$, $p= 0.05$) in EC users. Additionally, when EC users and cigarette smokers were pooled together, vaping episodes/cigarettes per day correlated with interleukin-6 levels ($r_s= 0.86$, $p= 0.006$). **Conclusion:** This is the first PET imaging study to compare lung inflammation between EC and cigarette users *in vivo*. We found preliminary evidence EC users had greater pulmonary inflammation than cigarette smokers and never smoke/vape controls, with a positive association between pulmonary and peripheral measures of inflammation.

Keywords: Electronic cigarettes, cigarettes, PET, ^{18}F -NOS, inflammation

INTRODUCTION

Tobacco use is the world's leading preventable cause of morbidity and mortality, accounting for more than 8 million deaths annually (1). Although public awareness of smoking-related risks has increased and tobacco smoking has declined, electronic cigarette (EC) use has increased dramatically, particularly among youth and young adults (1–3). The increase in EC use is partially driven by the assumption that ECs are safer than conventional cigarettes. Although ECs are often advertised as an alternative smoking cessation tool (4,5), their long-term effectiveness and safety have not been rigorously evaluated (6,7). Given the emergence of the EC or Vaping Product-Associated Lung Injury epidemic (8), EC use has become a major public health concern, and the adverse pulmonary effects of EC use remain unclear.

ECs deliver nicotine by heating e-liquids containing nicotine in a vegetable glycerin/propylene glycol vehicle with flavorings that are vaporized and inhaled, thus delivering nicotine without combusting tobacco. Although the propylene glycol and vegetable glycerin found in e-liquids are regarded as “safe” by the United States Food and Drug Administration, e-aerosols contain tobacco-specific nitrosamines, metals, polycyclic aromatic hydrocarbons, and volatile organic compounds that are known toxicants and carcinogens (9). As with smoking, several EC-related compounds are associated with inflammation, altered innate immune response, oxidative stress, and cytotoxicity (9–11). However, the existing human literature on the pulmonary effects of EC use is limited and comprised mainly of studies that use invasive approaches (e.g., induced sputum, bronchoalveolar lavage) that do not adequately assess the impact of EC use on the lungs.

Positron emission tomography (PET) imaging has been used to quantify and track inflammatory responses associated with smoking and EC use *in vivo* without the need for invasive diagnostic studies (12,13). PET with ¹⁸F-fluorodeoxyglucose (¹⁸F-FDG) has been used

extensively to detect enhanced glucose metabolic activity of activated immune cells in inflammatory diseases, including pneumonia (14), cystic fibrosis (14), and chronic obstructive pulmonary disease (COPD) (15). Although associations between ^{18}F -FDG quantification and inflammation have been observed, biological processes, including fibrosis and neoplasia, utilize glucose and limit the specificity of ^{18}F -FDG (16). PET radiotracers targeting the 18 kDa translocator protein, also known as the peripheral benzodiazepine receptor, have also been used to measure pulmonary inflammation (17,18). These radiotracers were initially considered putative markers of neuroinflammation; however, their specificity for inflammation is limited (19). Thus, recent efforts have focused on imaging specific aspects of immune regulation and response, such as nitric oxide synthase (NOS) enzymes, with promising results (16,20).

Nitric oxide (NO) plays an important role in immune regulation and is produced by three NOS enzymes: neuronal NOS, endothelial NOS, and inducible NOS (iNOS) (21). iNOS is associated with acute and chronic inflammatory diseases, including asthma and COPD (22,23), and is expressed in normal lung epithelium (24). Convergent evidence indicates that iNOS plays a central role in mediating inflammation in combustible cigarette smokers, thereby contributing to smoking-related lung diseases. Preclinical models show that chronic exposure to cigarette smoke increases iNOS expression (25), whereas pharmacological inhibition of iNOS reverses tobacco-induced lung disease (26). Additionally, preclinical research has provided a mechanistic link between iNOS expression in the lung and inflammatory lung diseases (26,27). These findings strongly support iNOS as a mechanistically relevant target for molecular imaging of lung inflammation and inflammatory lung diseases.

The PET radiotracer ^{18}F -6-(1/2)(2-fluoro-propyl)-4-methylpyridin-2-amine (^{18}F -NOS) permits the visualization and measurement of *in vivo* iNOS expression (16,28). ^{18}F -NOS is a radiolabeled version of a reversible iNOS inhibitor with better selectivity than other NOS enzymes

(28). ^{18}F -NOS has been validated in an animal model of lipopolysaccharide-induced lung injury (29) and was used successfully to image iNOS expression in humans to characterize oxidative stress and inflammation in the heart and lungs (16,28). This study uses ^{18}F -NOS PET lung imaging to quantify differences in iNOS expression among EC users, cigarette smokers, and never smoke/vape controls. Based on preclinical research showing that exposure to e-liquid vapor and cigarette smoke increases iNOS expression (25,30), we hypothesized that EC users and cigarette smokers would show greater pulmonary iNOS uptake than never smoke/vape controls. We also assessed blood/plasma inflammatory biomarker concentrations (tumor necrosis factor- α (TNF- α), interleukin (IL)-6, C-reactive protein (CRP)) and examined their association with ^{18}F -NOS PET lung imaging parameters.

MATERIALS AND METHODS

Participants

The study protocol was approved by the University of Pennsylvania Institutional Review Board and conducted in compliance with the Health Insurance Portability and Accountability Act under exploratory Investigational New Drug #140,976 for ^{18}F -NOS. Participants were recruited via local print media, social media, and previous research studies. Interested individuals completed a brief telephone screen and, if eligible, completed an in-person intake session during which they provided written informed consent and were screened for eligibility. Twenty-four participants underwent screening, including a physical examination, medical history, routine clinical laboratory tests, and toxicologic urine analysis. Briefly, exclusion criteria included history or evidence of significant medical disorders, a lifetime DSM-5 diagnosis of a psychiatric or substance use disorder (except tobacco use disorder for EC users and cigarette smokers), a positive urine drug screen, use of inhaled or oral corticosteroids or anti-inflammatory medications,

and a past-month history of lung trauma or active lung infection that could impact the uptake of ^{18}F -NOS. All female participants had a negative pregnancy test on the scanning day before receiving the radiotracer. EC users vaped nicotine, and cigarette smokers smoked daily for the past six months. Current smoking status was confirmed by carbon monoxide levels greater than 10 parts per million (ppm) and urine cotinine levels greater than 150 ng/mL. Fifteen age- and sex-matched participants (5 exclusive EC users [mean age=27 \pm 7], 5 cigarette smokers [mean age 35 \pm 9], and 5 never smoke/vape controls [mean age=28 \pm 7]), comprising 2 women and 3 men in each group, met eligibility criteria and completed the study (Supplementary Figure 1).

Before scanning, participants completed the Hospital Depression and Anxiety Scale (31) to assess symptoms of depression and anxiety. EC users completed measures of vaping behavior, including the Penn State Electronic Cigarette Dependence Index (32), and cigarette smokers completed measures of tobacco smoking behavior, including the Fagerström Test for Cigarette Dependence (33). A blood sample was obtained to measure blood/plasma cytokine concentrations (TNF- α , IL-6, and CRP). Participants underwent ^{18}F -NOS dynamic PET/CT thorax imaging with venous blood sampling.

Data Acquisition

The PET radiotracer ^{18}F -NOS was synthesized as previously described (28). Participants were scanned with a Philips Ingenuity PET/CT scanner (Philips Healthcare, Cleveland, OH, USA), which has a 5-mm full-width at half maximum PET spatial resolution and an 18-cm axial field of view (34). For each scan, thoracic scanning field of view to best include the heart and lungs was determined by a Nuclear Medicine physician. After a low-dose attenuation-correction CT scan, a 1-h PET dynamic acquisition was started at the time of an intravenous bolus injection of ^{18}F -NOS (199 \pm 27 MBq) with the following framing schedule: 24 \times 5-s, 6 \times 10-s, 3 \times 20-s, 2 \times 30-s, 5 \times 60-s, and 10 \times 5-min frames. Based on published effective dose estimates of 15.9 $\mu\text{Sv}/\text{MBq}$ for ^{18}F -NOS,

199 MBq delivers an effective dose of 3.16 mSv with maximum critical dose to the urinary bladder wall of 19.0 mSv (28). The attenuation-correction CT images were reconstructed into PET images using a previously described list-mode, blob-based, ordered-subsets, maximum-likelihood, expectation-maximization algorithm, including flight-time and physical-data corrections (34). The radiologist who reviewed the images and the data analyst were blind to participant group status.

Metabolite Analysis

Venous blood was sampled at approximately 2, 5, 10, 15, 30, 45, and 60 min after injection to measure radiometabolites. The whole-blood and plasma activity concentrations were counted using a WIZARD² 2480 gamma counter (Perkin Elmer, Waltham, MA). Acetonitrile-treated plasma supernatant was analyzed in a 1260 Infinity Series (Agilent Technologies, Santa Clara, CA) high-performance liquid chromatography system using an Agilent ZORBAX StableBond C18 column via a mobile phase of 73% 0.1 M ammonium formate buffer and 27% methanol. The resulting plasma-to-whole blood ratio as a function of time was used to convert the image-derived whole blood input function into a plasma input function. The resulting parent PET radiotracer fraction as a function of time and the plasma input function were inputted for subsequent kinetic analysis.

Volumes of Interest

Whole-blood pool time activity curves (TACs) were measured using 1 cm³ peak volumes of interest (VOIs) within 2-cm diameter spherical search VOIs within the pulmonary artery, as this blood pool is sufficiently large to minimize partial volume effects and located immediately before blood enters the lungs (Figure 1). Lung uptake TACs were extracted from all lung tissue in the PET field of view (Figure 1).

Kinetic Analysis

Three models of kinetic analysis were compared for estimating the total volume of distribution (V_T) from the observed reversible tracer binding: graphical Logan plot (35), 1-tissue compartment (1TC), and 2-tissue compartment (2TC). The 2TC model, with an average whole lung Akaike information criterion (AIC) (36,37) of 184 ± 31 , was selected over the 1TC, with a corresponding AIC of 295 ± 24 , based on the 2TC having the lower, and therefore better, AIC score. V_T values estimated via the Logan and 2TC models were similar ($R^2 = 0.99$). As expected, V_T values from Logan plots were biased lower than when using the 2TC model, with the magnitude of the Logan plot V_T bias decreasing with increases in the duration of the PET acquisition. Thus, we used the 2TC model to quantify tracer uptake to avoid having metrics dependent on the PET scan duration.

Two approaches for blood volume fraction (v_B) were examined for each model: fixed at 0.15 and floating between 0.05 and 0.3. Floating v_B resulted in the least model variability. Kinetic analyses using a 2TC model with a floated lung blood volume fraction (v_B) were performed to estimate V_T , transport into the first tissue compartment (K_1), distribution volume of the first tissue compartment (K_1/k_2), and non-displaceable binding potential (BP_{ND}) via Pmod image analysis software (Pmod v3.7, PMOD Technologies Ltd., Zurich, Switzerland) using the combined lung TAC and PET image-derived plasma input function from the pulmonary artery blood pool (see Figure 1) (38). Kinetic analyses were based on the first 40 min of PET acquisition to allow a consistent analysis of all participants' data after one participant's excessive motion resulted in unevaluable PET images after 40 minutes.

Statistical Analysis

All statistical tests were two-sided. Non-parametric Mann-Whitney and Kruskal-Wallis tests were used to assess group differences. Spearman rank-order correlations measured the

strength and direction of associations between inflammatory biomarkers, nicotine use behaviors (cigarettes per day for cigarette smokers; vaping episodes per day for EC users), and imaging parameters.

RESULTS

On average, EC users reported 7 ± 4 vaping episodes/day, with Penn State Electronic Cigarette Dependence Index scores of 6 ± 4 , indicating moderate-to-high levels of EC dependence. Cigarette smokers reported smoking 8 ± 4 cigarettes/day, with Fagerström Test for Cigarette Dependence scores of 5 ± 2 , indicating moderate levels of cigarette dependence. There were no significant group differences in age, depression and anxiety scores, injected mass radioactivity dose or plasma-free fraction.

Selection of the pulmonary artery to measure the blood input function is supported by the example fused PET/CT images in Figure 1, where the distribution of ^{18}F -NOS before entry into the lungs indicates ^{18}F -NOS entering the right atrium followed by the pulmonary artery before lung entry and subsequent transport to lungs followed by the left ventricle. Figure 2 shows average lung ^{18}F -NOS uptake for all participants as a function of time. Table 1 presents kinetic analysis results, where the average estimate of lung blood volume fraction (vB) of 0.15 ± 0.02 is consistent with the reported normal lung vB range of 0.14 to 0.19 from ^{18}F -FDG PET/CT scans (39).

^{18}F -NOS BP_{ND} values differed significantly between groups, $H(2) = 7.50$, $p = 0.02$ (Figure 3). Post-hoc comparisons revealed that EC users had higher BP_{ND} values than cigarette smokers ($p = 0.03$) and healthy never smoke/vape controls ($p = 0.01$). ^{18}F -NOS V_{T} and K_1 values did not differ between groups (p 's > 0.09).

Peripheral inflammatory biomarker concentrations did not differ between groups (p 's > 0.16). Spearman's rank-order correlations examined the associations between daily smoking/vaping behavior, inflammatory biomarker concentrations, and imaging parameters. There was a positive correlation among EC users between ^{18}F -NOS BP_{ND} and TNF- α concentration ($r_s = 0.87$, $p = 0.05$; Supplementary Figure 2). Among EC users and cigarette smokers, cigarettes per day and vaping episodes per day correlated with IL-6 levels ($r_s = 0.89$, $p = 0.001$; Supplementary Figure 3). No other correlations were statistically significant.

DISCUSSION

EC use has increased dramatically, particularly among adolescents and young adults. Consequently, well-controlled studies are urgently needed to examine and compare the effects of EC use and cigarette smoking. The existing literature mainly comprises cell culture studies or *in vivo* animal studies. A few studies examine the effects of EC use on the human lung based on invasive approaches that do not assess the global burden of EC use on the lungs. This preliminary study addresses these gaps by using non-invasive, ^{18}F -NOS PET lung imaging to quantify and compare lung inflammation in exclusive EC users, exclusive cigarette smokers, and never smoke/vape controls. Our preliminary ^{18}F -NOS PET findings show that EC users have similar delivery of ^{18}F -NOS to the lung tissue and iNOS availability similar to that of cigarette smokers and never smoke/vape controls. However, ^{18}F -NOS BP_{ND} was significantly higher in the EC group than in cigarette smokers and controls. Moreover, ^{18}F -NOS BP_{ND} in EC users was associated with the pro-inflammatory cytokine TNF- α . Cigarettes and vaping episodes per day correlated with IL-6 levels among cigarette smokers and EC users. This is the first PET lung imaging study demonstrating that EC users show a unique PET lung phenotype associated with known inflammatory biomarkers.

Although we did not see the expected increase in ^{18}F -NOS uptake in cigarette smokers, findings are consistent with recent work that used bronchoscopy to isolate alveolar macrophages from bronchoalveolar lavage samples in smokers, EC users, and never-smokers and found that EC users showed greater iNOS expression in alveolar macrophages than in smokers or never-smokers (40). Animal and human studies show that iNOS expression is induced in most cell types upon exposure to inflammatory stimuli (41) and is associated with increased pulmonary NO (42). NO mediates neutrophil and macrophage actions that are thought to contribute to pulmonary oxidant stress and acute lung injury (43). Thus, our findings suggest that EC use may alter pulmonary oxidative stress responses and predispose them to acute lung injury.

Although groups showed similar levels of inflammatory biomarkers, EC users showed positive associations between ^{18}F -NOS PET imaging parameters and TNF- α concentration. TNF- α is a pro-inflammatory cytokine produced by macrophages and secreted by neutrophil granulocytes at sites of injury (44) and is involved in the inflammatory cascade of acute lung injury (45). Indeed, studies show that pro-inflammatory cytokines induce iNOS expression in human alveolar cells in response to exposure to fine particulate matter (46). As such, our findings provide additional evidence of the altered immune responses in the lungs of EC users.

Several limitations should be considered. First, we did not account for vaping topography (i.e., how an EC is used, including puff duration, puff volume, and EC device and power settings). These factors are important in differential exposure to nicotine and toxicants among EC users (47). While we used individually measured PET radiotracer parent fractions as a function of time to correct for the presence of radiolabelled metabolites in the blood, we could not separate lung ^{18}F -NOS uptake due to binding of parent ^{18}F -NOS from any binding of radiolabelled metabolites. Huang et al. asserted, “because of [the metabolite’s] polarity, this metabolite is most likely excluded by the lung endothelium from entering the lung parenchyma” (16). Impacts of any lung

binding of radiolabelled metabolites on estimates of ^{18}F -NOS BP_{ND} will likely be inversely related to the validity of the assumption that polar ^{18}F -NOS metabolites cannot penetrate lung endothelium. To date, no studies provide information on the reproducibility of the ^{18}F -NOS PET assay; however, previous research showed consistent findings in left and right lung ^{18}F -NOS parameters (16). In addition, the sample sizes are small, so additional larger studies are needed to replicate these findings and provide greater statistical power for secondary analyses.

CONCLUSION

Using rigorous quantitative methods and a global technique to examine pulmonary oxidative stress, we find evidence that EC use causes a unique inflammatory response in the lungs, reflected by PET measures of iNOS expression and correlations with inflammatory biomarker concentrations. Future work is needed to elucidate the effect of EC use on respiratory health, especially the effects of chronic EC use.

ACKNOWLEDGMENTS

The study was supported by the National Heart, Lung, and Brain Institute (R21HL144673), the National Institute on Drug Abuse (P30DA046345), the National Center for Advancing Translational Sciences of the National Institutes of Health under Award Number UL1TR001878, and in part by the Institute for Translational Medicine and Therapeutics' (ITMAT) Transdisciplinary Program in Translational Medicine and Therapeutics.

DISCLOSURES

Dr. Kranzler is a member of advisory boards for Dicerna Pharmaceuticals, Sophrosyne Pharmaceuticals, and Enthion Pharmaceuticals; a consultant to Sobrera Pharmaceuticals; recipient of grant funds and medication supplies from Alkermes for an investigator-initiated study; a member of the American Society of Clinical Psychopharmacology's Alcohol Clinical Trials Initiative, which was supported by Alkermes, Dicerna, Ethypharm, Lundbeck, Mitsubishi, and Otsuka; and a holder of U.S. patent 10,900,082 titled: "Genotype-guided dosing of opioid agonists," issued 26 January 2021. Drs. Dubroff, Doot, and Mach have received support from the Michael J. Fox Foundation. All other authors do not have disclosures to report.

KEY POINTS

QUESTION: What are the effects of e-cigarette use on pulmonary inflammation compared to combustible cigarette use and never smoking/vaping, as measured with ^{18}F -NOS PET imaging?

PERTINENT FINDINGS: In this preliminary PET imaging study, e-cigarette users showed greater ^{18}F -NOS non-displaceable binding potential (BP_{ND}) than cigarette smokers and never smoke/vape controls. ^{18}F -NOS BP_{ND} significantly correlated with the pro-inflammatory cytokine TNF- α in e-cigarette users. Additionally, when e-cigarette users and cigarette smokers were pooled together, vaping episodes/cigarettes per day correlated with IL-6 levels.

IMPLICATIONS FOR PATIENT CARE: Preliminary data indicate that e-cigarette users show a unique PET lung imaging phenotype associated with known pro-inflammatory cytokines, suggesting that e-cigarette use may increase pulmonary inflammation.

REFERENCES

1. WHO report on the global tobacco epidemic 2021: addressing new and emerging products. Geneva: World Health Organization; 2021. Licence: CC BY-NC-SA 3.0 IGO.
2. Wang TW, Gentzke AS, Neff LJ, et al. Disposable e-cigarette use among U.S. youth — an emerging public health challenge. *N Engl J Med*. 2021;384:1573-1576.
3. Miech R, Johnston L, O'Malley PM, Bachman JG, Patrick ME. Trends in adolescent vaping, 2017–2019. *N Engl J Med*. 2019;381:1490-1491.
4. Ioakeimidis N, Vlachopoulos C, Tousoulis D. Efficacy and safety of electronic cigarettes for smoking cessation: a critical approach. *Hellenic J Cardiol*. 2016;57:1-6.
5. Kalkhoran S, Glantz SA. E-cigarettes and smoking cessation in real-world and clinical settings: a systematic review and meta-analysis. *Lancet Respir Med*. 2016;4:116-128.
6. Pisinger C, Døssing M. A systematic review of health effects of electronic cigarettes. *Prev Med*. 2014;69:248-260.
7. Lundbäck B, Katsaounou P, Lötvall J. The up-rise in e-cigarette use – friend or foe? *Respir Res*. 2016;17:52, s12931-016-0371-2.
8. Cherian SV, Kumar A, Estrada-Y-Martin RM. E-Cigarette or Vaping Product-Associated Lung Injury: a review. *Am J Med*. 2020;133:657-663.
9. Goniewicz ML, Smith DM, Edwards KC, et al. Comparison of nicotine and toxicant exposure in users of electronic cigarettes and combustible cigarettes. *JAMA Netw Open*. 2018;1:e185937.

10. Shields PG, Berman M, Brasky TM, et al. A review of pulmonary toxicity of electronic cigarettes in the context of smoking: a focus on inflammation. *Cancer Epidemiol Biomark Prev.* 2017;26:1175-1191.
11. Reidel B, Radicioni G, Clapp PW, et al. E-cigarette use causes a unique innate immune response in the lung, involving increased neutrophilic activation and altered mucin secretion. *Am J Respir Crit Care Med.* 2018;197:492-501.
12. Tong L, Sui Y, Jiang S, Yin Y. The association between lung fluorodeoxyglucose metabolism and smoking history in 347 healthy adults. *J Asthma Allergy.* 2021;14:301-308.
13. Sahota A, Naidu S, Jacobi A, et al. Atherosclerosis inflammation and burden in young adult smokers and vapers measured by PET/MR. *Atherosclerosis.* 2021;325:110-116.
14. Tateishi U, Hasegawa T, Seki K, Terauchi T, Moriyama N, Arai Y. Disease activity and 18F-FDG uptake in organising pneumonia: semi-quantitative evaluation using computed tomography and positron emission tomography. *Eur J Nucl Med Mol Imaging.* 2006;33:906-12.
15. Jones HA, Marino PS, Shakur BH, Morrell NW. In vivo assessment of lung inflammatory cell activity in patients with COPD and asthma. *Eur Respir J.* 2003;21:567-73.
16. Huang HJ, Isakow W, Byers DE, et al. Imaging pulmonary inducible nitric oxide synthase expression with PET. *J Nucl Med.* 2015;56:76-81.
17. Hatori A, Yui J, Yamasaki T, et al. PET imaging of lung inflammation with [18F]FEDAC, a radioligand for translocator protein (18 kDa). *PLoS One.* 2012;7:e45065.

18. Branley HM, du Bois RM, Wells AU, Jones HA. Peripheral-type benzodiazepine receptors in bronchoalveolar lavage cells of patients with interstitial lung disease. *Nucl Med Biol.* 2007;34:553-8.
19. Notter T, Coughlin JM, Sawa A, Meyer U. Reconceptualization of translocator protein as a biomarker of neuroinflammation in psychiatry. *Mol Psychiatry.* 2018;23:36-47.
20. Koch A, Burgschweiger A, Herpel E, et al. Inducible NO synthase expression in endomyocardial biopsies after heart transplantation in relation to the postoperative course. *Eur J Cardiothorac Surg.* 2007;32:639-43.
21. Alderton WK, Cooper CE, Knowles RG. Nitric oxide synthases: structure, function and inhibition. *Biochem J.* 2001;357:593-615.
22. Islam T, Breton C, Salam MT, et al. Role of inducible nitric oxide synthase in asthma risk and lung function growth during adolescence. *Thorax.* 2010;65:139-145.
23. Csoma B, Bikov A, Nagy L, et al. Dysregulation of the endothelial nitric oxide pathway is associated with airway inflammation in COPD. *Respir Res.* 2019;20:156.
24. Guo FH, De Raeve HR, Rice TW, Stuehr DJ, Thunnissen FB, Erzurum SC. Continuous nitric oxide synthesis by inducible nitric oxide synthase in normal human airway epithelium in vivo. *Proc Natl Acad Sci U A.* 1995;92:7809-13.
25. Khanna A, Guo M, Mehra M, Royal W. Inflammation and oxidative stress induced by cigarette smoke in Lewis rat brains. *J Neuroimmunol.* 2013;254:69-75.
26. Seimetz M, Parajuli N, Pichl A, et al. Inducible NOS inhibition reverses tobacco-smoke-induced emphysema and pulmonary hypertension in mice. *Cell.* 2011;147:293-305.

27. Bhandari V, Choo-Wing R, Chapoval SP, et al. Essential role of nitric oxide in VEGF-induced, asthma-like angiogenic, inflammatory, mucus, and physiologic responses in the lung. *Proc Natl Acad Sci U A*. 2006;103:11021-6.
28. Herrero P, Laforest R, Shoghi K, et al. Feasibility and dosimetry studies for ¹⁸F-NOS as a potential PET radiopharmaceutical for inducible nitric oxide synthase in humans. *J Nucl Med*. 2012;53:994-1001.
29. Zhou D, Lee H, Rothfuss JM, et al. Design and synthesis of 2-amino-4-methylpyridine analogues as inhibitors for inducible nitric oxide synthase and in vivo evaluation of [¹⁸F]6-(2-fluoropropyl)-4-methyl-pyridin-2-amine as a potential PET tracer for inducible nitric oxide synthase. *J Med Chem*. 2009;52:2443-53.
30. Kuntic M, Oelze M, Steven S, et al. Short-term e-cigarette vapour exposure causes vascular oxidative stress and dysfunction: evidence for a close connection to brain damage and a key role of the phagocytic NADPH oxidase (NOX-2). *Eur Heart J*. 2020;41:2472-2483.
31. Zigmond AS, Snaith RP. The Hospital Anxiety and Depression Scale. *Acta Psychiatr Scand*. 1983;67:361-370.
32. Foulds J, Veldheer S, Yingst J, et al. Development of a questionnaire for assessing dependence on electronic cigarettes among a large sample of ex-smoking E-cigarette users. *Nicotine Tob Res*. 2015;17:186-92.
33. Fagerstrom K. Determinants of tobacco use and renaming the FTND to the Fagerstrom Test for Cigarette Dependence. *Nicotine Tob Res*. 2012;14:75-8.

34. Kolthammer JA, Su K-H, Grover A, Narayanan M, Jordan DW, Muzic RF. Performance evaluation of the Ingenuity TF PET/CT scanner with a focus on high count-rate conditions. *Phys Med Biol.* 2014;59:3843-3859.
35. Logan J, Fowler JS, Volkow ND, et al. Graphical analysis of reversible radioligand binding from time—activity measurements applied to [*N* - ¹¹C-Methyl]-(-)-cocaine PET studies in human subjects. *J Cereb Blood Flow Metab.* 1990;10:740-747.
36. Akaike H. Likelihood of a model and information criteria. *J Econom.* 1981;16:3-14.
37. Golla SSV, Adriaanse SM, Yaqub M, et al. Model selection criteria for dynamic brain PET studies. *EJNMMI Phys.* 2017;4:30.
38. Doot R, Young A, Dominguez T, et al. Blood pool selection for quantifying lung inflammation via [18F]NOS uptake in nicotine users and healthy humans. *J Nucl Med.* 2020;61:205-205.
39. Holman BF, Cuplov V, Millner L, et al. Improved correction for the tissue fraction effect in lung PET/CT imaging. *Phys Med Biol.* 2015;60:7387-7402.
40. Davis ES, Ghosh A, Coakley RD, et al. Chronic e-cigarette exposure alters human alveolar macrophage morphology and gene expression. *Nicotine Tob Res.* 2022;24:395-399.
41. Zamora R, Vodovotz Y, Billiar TR. Inducible nitric oxide synthase and inflammatory diseases. *Mol Med.* 2000;6:347-373.
42. Mehta A, Guidot D. Alcohol and the lung. *Alcohol Res Curr Rev.* 2017;38:243-254.
43. Chow C-W, Herrera Abreu MT, Suzuki T, Downey GP. Oxidative stress and acute lung injury. *Am J Respir Cell Mol Biol.* 2003;29:427-431.

44. Tonstad S, Cowan JL. C-reactive protein as a predictor of disease in smokers and former smokers: a review. *Int J Clin Pract.* 2009;63:1634-1641.
45. Cross LJM, Matthay MA. Biomarkers in acute lung injury: insights into the pathogenesis of acute lung injury. *Crit Care Clin.* 2011;27:355-377.
46. Niu X, Ho KF, Hu T, et al. Characterization of chemical components and cytotoxicity effects of indoor and outdoor fine particulate matter (PM_{2.5}) in Xi'an, China. *Environ Sci Pollut Res.* 2019;26:31913-31923.
47. Lee YO, Nonnemaker JM, Bradfield B, Hensel EC, Robinson RJ. Examining daily electronic cigarette puff topography among established and nonestablished cigarette smokers in their natural environment. *Nicotine Tob Res.* 2018;20:1283-1288.

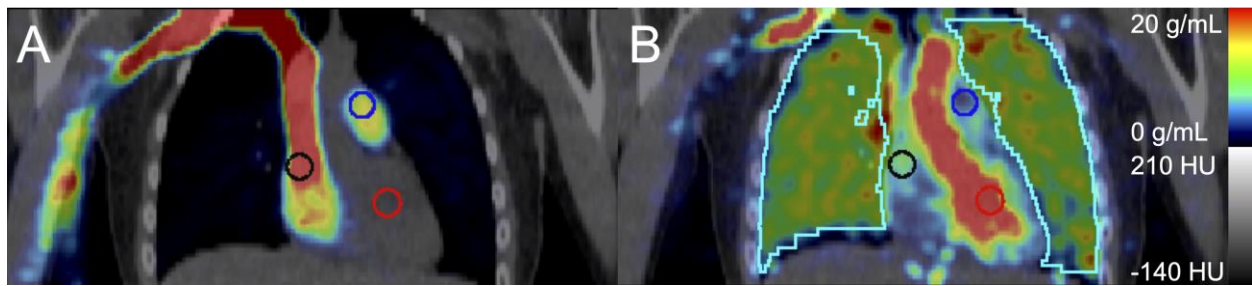


FIGURE 1. Representative fused coronal PET/CT images after injecting 207 MBq ^{18}F -NOS with 2-cm diameter spherical blood pool search volumes of interest in the right atrium (black), pulmonary artery (blue), and left ventricle (red) with (A) PET summed uptake 0-15 s post-injection and (B) PET summed 37 to 42 seconds post-injection with lung volume of interest (cyan).

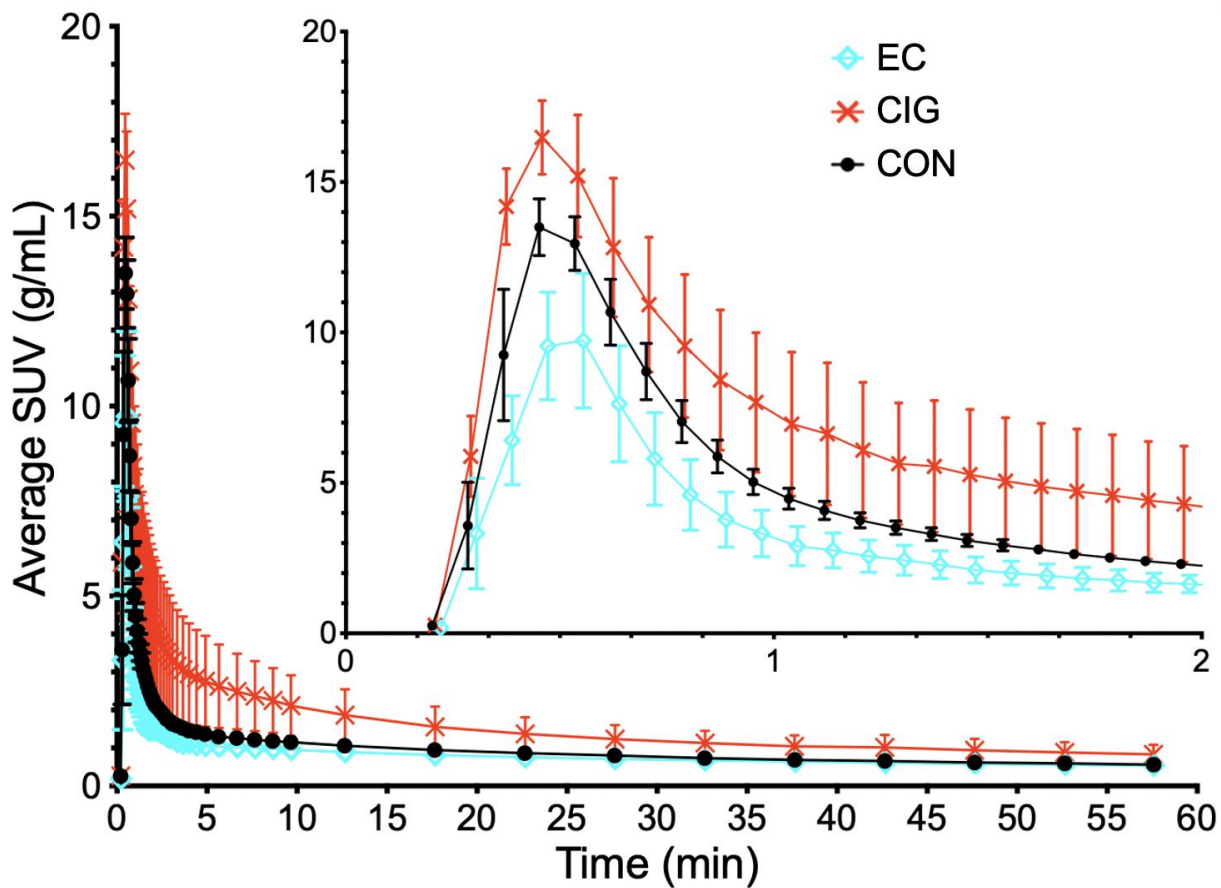


FIGURE 2. Average lung ^{18}F -NOS uptake for each group as functions of time with standard deviation error bars. EC = E-Cigarette Users, CIG = Cigarette Smokers, CON = Never Smoke/Vape Controls, SUV = standard uptake value.

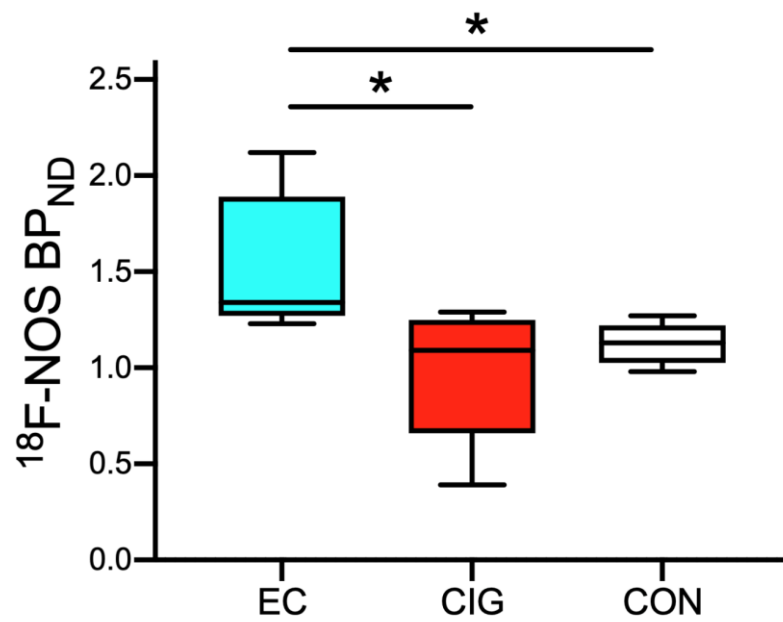


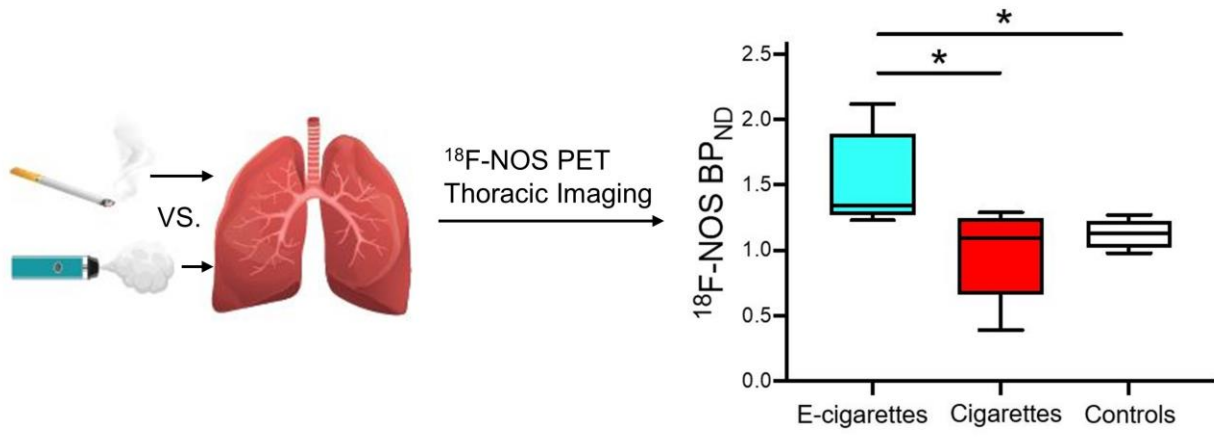
FIGURE 3. Boxplot of $^{18}\text{F-NOS BP}_{\text{ND}}$ by Group. EC Users show higher $^{18}\text{F-NOS BP}_{\text{ND}}$ than never smoke/vape controls ($p = 0.01$) and cigarette smokers ($p = 0.03$). BP_{ND} = non-displaceable binding potential. EC = E-Cigarette Users, CIG = Cigarette Smokers, CON = Never Smoke/Vape Controls. * $p < 0.05$

TABLE 1Individual and cohort gender and ^{18}F -NOS kinetic measures

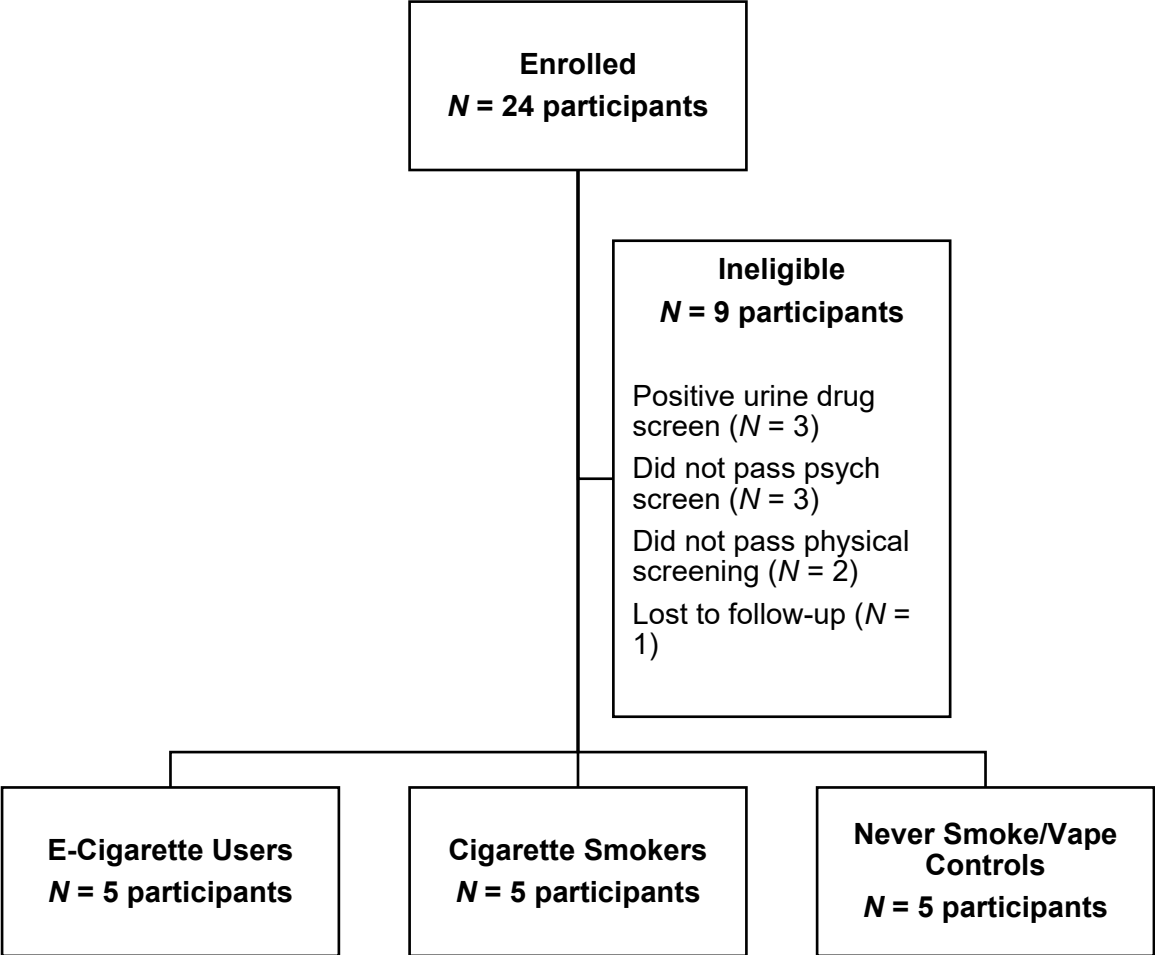
ID	M/F	V_T	K_1	K_1/k_2	BP_{ND}	v_B
<u>Electronic cigarette users (EC)</u>						
EC-07	F	1.17	1.62	0.51	1.31	0.15
EC-10	M	0.63	1.42	0.28	1.23	0.16
EC-13	F	0.99	1.58	0.42	1.34	0.18
EC-20	M	1.20	2.67	0.39	2.12	0.18
EC-23	M	0.83	1.26	0.31	1.66	0.13
<u>Combustible cigarette users (CIG)</u>						
CIG-12	M	1.10	2.71	0.57	0.93	0.14
CIG-14	M	4.74	2.29	3.42	0.39	0.14
CIG-17	M	1.14	3.24	0.52	1.21	0.16
CIG-22	F	1.45	2.70	0.66	1.29	0.11
CIG-24	F	1.06	1.62	0.51	1.09	0.15
<u>Never users (NU)</u>						
NU-01	F	1.15	1.95	0.58	0.98	0.18
NU-03	M	1.04	1.85	0.48	1.17	0.15
NU-05	M	0.91	1.37	0.40	1.27	0.15
NU-06	F	1.53	3.19	0.74	1.07	0.17
NU-09	M	1.18	1.62	0.56	1.13	0.13
EC (n=5):		0.97 ± 0.24	1.71 ± 0.56	$0.38 \pm 0.09^*$	$1.53 \pm 0.37^*$	0.16 ± 0.02
CIG (n=5):		1.90 ± 1.60	2.51 ± 0.60	1.13 ± 1.28	0.98 ± 0.36	0.14 ± 0.02
NEVER USERS (n=5):		1.16 ± 0.23	1.99 ± 0.70	0.55 ± 0.13	1.12 ± 0.11	0.16 ± 0.02
All (n=15):		1.34 ± 0.97	2.07 ± 0.67	0.69 ± 0.77	1.21 ± 0.37	0.15 ± 0.02
<i>p-value</i>		0.36	0.09	0.03	0.02	0.31

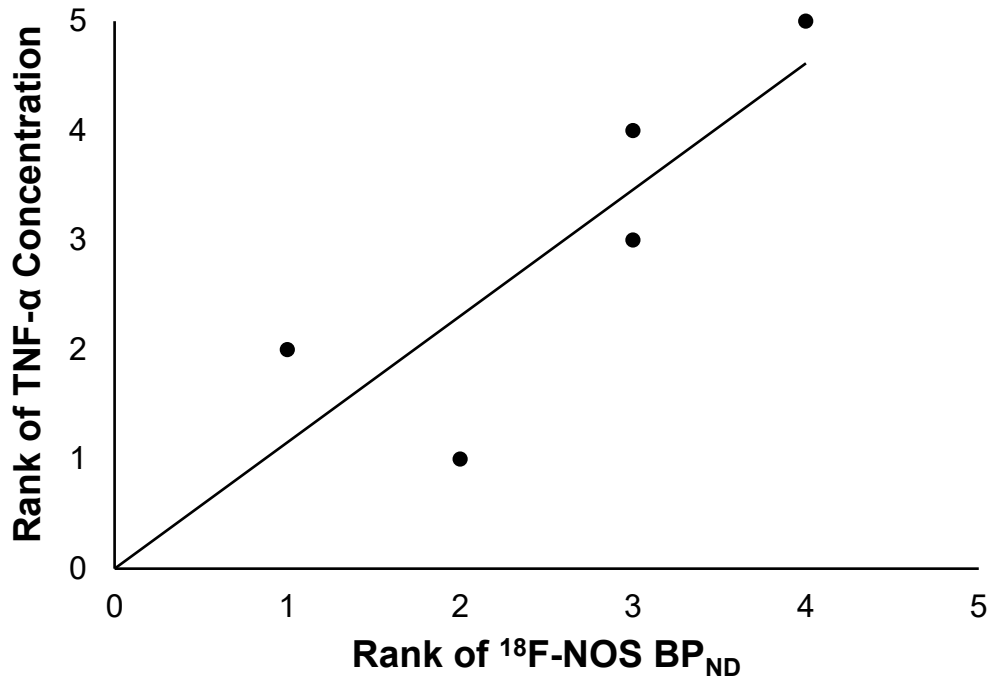
ID = participant study identification number; M/F = male/female biological sex; V_T = total volume of distribution; K_1 = delivery rate constant; K_1/k_2 = distribution volume of the first tissue compartment; BP_{ND} = non-displaceable binding potential; v_B = blood volume fraction. Data are mean values and mean \pm standard deviation. *p*-value from Kruskal-Wallis test comparing the three groups. * $p < 0.05$ on comparison between EC and Never users.

Graphical Abstract

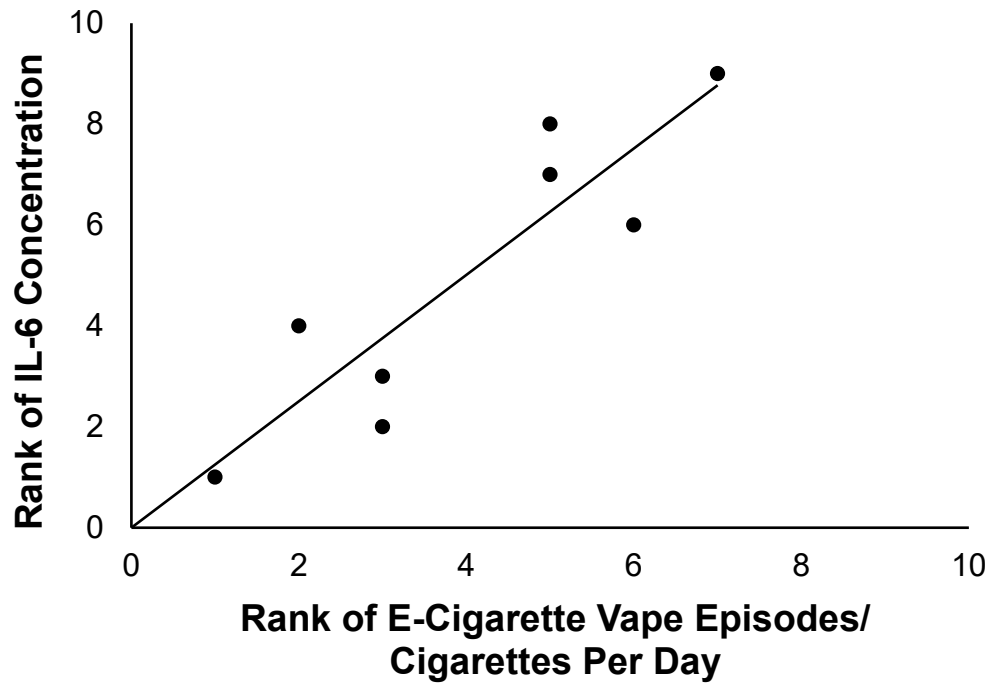


Supplementary Figure 1: STARD flow diagram





Supplementary Figure 2. Scatterplot demonstrating the rank-order correlation between ¹⁸F-NOS non-displaceable binding potential and tumor necrosis factor-α concentration in e-cigarette users ($r_s = 0.87$, $p = 0.05$).



Supplementary Figure 3. Scatterplot demonstrating the rank-order correlation between e-cigarette vape episodes/cigarettes per day and interleukin (IL)-6 concentration in e-cigarette and combustible cigarette users ($r_s = 0.89$, $p = 0.001$).